



**HAL**  
open science

## Deep conservation of bivalve nacre proteins highlighted by shell matrix proteomics of the *Unionoida Elliptio complanata* and *Villosa lienosa*.

Benjamin Marie, Jaison Arivalagan, Lucrèce Mathéron, Gérard Bolbach, Sophie Berland, Arul Marie, Frédéric Marin

### ► To cite this version:

Benjamin Marie, Jaison Arivalagan, Lucrèce Mathéron, Gérard Bolbach, Sophie Berland, et al.. Deep conservation of bivalve nacre proteins highlighted by shell matrix proteomics of the *Unionoida Elliptio complanata* and *Villosa lienosa*.. *Journal of the Royal Society Interface*, 2017, 14 (126), pp.20160846. 10.1098/rsif.2016.0846 . hal-01470764

**HAL Id: hal-01470764**

**<https://hal.science/hal-01470764>**

Submitted on 27 Mar 2017

**HAL** is a multi-disciplinary open access archive for the deposit and dissemination of scientific research documents, whether they are published or not. The documents may come from teaching and research institutions in France or abroad, or from public or private research centers.

L'archive ouverte pluridisciplinaire **HAL**, est destinée au dépôt et à la diffusion de documents scientifiques de niveau recherche, publiés ou non, émanant des établissements d'enseignement et de recherche français ou étrangers, des laboratoires publics ou privés.

1 **Deep conservation of bivalve nacre proteins highlighted by shell matrix**  
2 **proteomics of the Unionoida *Elliptio complanata* and *Villosa lienosa***

3  
4 Benjamin Marie<sup>1,\*</sup>, Jaison Arivalagan<sup>1</sup>, Lucrece Mathéron<sup>2</sup>, Gérard Bolbach<sup>2</sup>, Sophie Berland<sup>3</sup>,  
5 Arul Marie<sup>1</sup>, Frédéric Marin<sup>4</sup>

6  
7 <sup>1</sup>UMR 7245 CNRS/MNHN Molécules de Communications et Adaptations des Micro-organismes, Muséum  
8 National d'Histoire Naturelle, Paris – France

9 <sup>2</sup>UMR 7203 CNRS/UPMC/ENS/INSERM Laboratoire des Biomolécules, Institut de Biologie Paris Seine,  
10 Université Pierre et Marie Curie, Paris – France

11 <sup>3</sup>UMR 7208 CNRS/MNHN/UPMC/IRD Biologie des Organismes Aquatiques et Ecosystèmes, Muséum  
12 National d'Histoire Naturelle, Paris - France

13 <sup>4</sup>UMR 6282 CNRS/uB Biogéosciences, Université de Bourgogne Franche-Comté (UB-FC), Dijon – France

14  
15 \*Author for correspondence

16 Benjamin Marie

17 Email: bmarie@mnhn.fr

18  
19 **Subject area:** biomaterials, biochemistry, evolution

20  
21 **Keywords:** biomineralization, shell nacre, proteomics, bivalve, organic matrix proteins,  
22 calcium carbonate.

23

24 The formation of the molluscan shell nacre is regulated to a large extent by a matrix of  
25 extracellular macromolecules that are secreted by the shell forming tissue, the mantle. This so  
26 called “calcifying matrix” is a complex mixture of proteins, glycoproteins and  
27 polysaccharides that is assembled and occluded within the mineral phase during the  
28 calcification process. The fine molecular basis that regulates nacre formation remains to be  
29 better characterized.

30 Noticeable advances in expressed tag sequencing of the freshwater mussels, such as *Elliptio*  
31 *complanata* and *Villosa lienosa*, provide a pre-requisite to further characterize the bivalve  
32 nacre proteins by a proteomic approach. In this study, we have identified a total of 48  
33 different proteins from the nacre insoluble matrices, 31 of which are common of the two  
34 species. Few of these proteins, such as PIF, MSI60, CA, shematrin-like, Kunitz-like, LamG,  
35 chitin-binding containing proteins, together with A-, D-, G-, M- and Q-rich proteins, appear to  
36 be analogues, if not true homologs, of proteins previously described from the pearl oyster or  
37 the edible mussel nacre matrices, thus constituting a remarkable list of deeply-conserved  
38 nacre protein set. This work constitutes a comprehensive nacre proteomic study of non-  
39 pteriomorphid bivalves that concretely gives us the opportunity to describe the molecular  
40 basis of deeply conserved biomineralization toolkit among nacreous shell-bearing bivalves,  
41 with regard to proteins associated to other shell microstructures, to that of other mollusc  
42 classes (gastropods, cephalopods) and finally, to other lophotrochozoans (brachiopods).

43

## 44 **1. Introduction**

### 45 (a) Mollusc shell biomineralization

46 The molluscan shell is a unique model for biomineralization and constitutes a remarkable  
47 example of a natural composite biomaterial synthesized at ambient temperature from polar to  
48 tropical environment. It is composed of one or two polymorphs of calcium carbonate (*i.e.*  
49 calcite and aragonite), generally assembled in superimposed CaCO<sub>3</sub> layers of different  
50 microstructures [1]. These different shell layer textures are produced under the control of  
51 specific extracellular matrices that are secreted by different zones of the external mantle  
52 epithelium [2]. These ‘cell-free’ matrices, mainly constituted of proteins, glycoproteins and  
53 polysaccharides, surround nascent CaCO<sub>3</sub> crystals and are incorporated into the shell  
54 crystalline architecture in growth. Although the organic matrix is quantitatively a minor  
55 component of the shell (0.1 to 5 wt-%), it is thought to play a central role in the formation and  
56 shaping of these biomineral structures [3-4]. Indeed, these matrix components have been  
57 shown to be involved in the organization of a spatially prearranged scaffold, the nucleation,  
58 the orientation and growth of calcium carbonate crystals and the inhibition of their growth [5].  
59 It has also been demonstrated that the nacre matrix controls the calcium carbonate polymorph  
60 [6] and that it exhibits cell-signalling properties [7-9].

61

### 62 (b) Nacre

63 Because of its extraordinary toughness, commercial value in jewelry and remarkable  
64 biocompatibility properties, nacre, so called the mother of pearl, is by far the most studied  
65 molluscan shell microstructure. Moreover, many authors consider it as the reference model  
66 for understanding how molluscs control the fine deposition of calcium carbonate layers [10].  
67 From a structural viewpoint, nacre is constituted by a regular superimposition of polygonal  
68 flat aragonitic tablets of about 0.5 μm thickness, embedded in a peripheral thin organic matrix  
69 [11]. Nacre constitutes also a fascinating object for the investigation of evolutionary  
70 processes, as it appeared early in the fossil record, during the Cambrian times [12-13], and  
71 kept almost unchanged until now. At present it is distributed in four mollusc classes,  
72 comprising cephalopods, gastropods, monoplacophorans and bivalves. In this latter group,  
73 nacre is widespread in paleotaxodont, pteriomorphid, paleoheterodont and anomalodesmata  
74 clades [14]. One key question consists in determining if similar shell nacre textures, present in  
75 these different taxa, are produced by homologous sets of protein assemblages, or not. Such  
76 information would provide us a better appreciation on the recruitment of nacre matrix proteins

77 in the Cambrian, on the evolutionary constraints exerted on these proteins, and finally, on the  
78 open debate on the unique or multiple inventions of nacre among molluscs.

79

### 80 (c) Nacre proteins

81 Since the initial description of the primary structure of a mollusc shell protein in 1996 [15],  
82 numerous nacre associated-proteins have been described so far mainly from three principal  
83 models, the pearl oyster [2;16] and the edible mussel for bivalves [17-18], and the abalone for  
84 gastropods [19]. Comparison of their respective nacre biomineralization toolkits from the  
85 pearl mussel *Pinctada maxima* and the abalone *Haliotis asinina* underlined unexpectedly very  
86 few sequence similarities, suggesting either that the bivalves and gastropods acquired  
87 independently the capacity to synthesize nacre, or that these proteins present rapid evolution  
88 rate, especially in abalone, leading to functional conservation of respective nacre shell matrix  
89 protein (SMP) sets with only limited primary structure similarities [20]. In bivalves, most of  
90 the published data for nacre proteins comes from the Pteriomorpha sub-class [2;16-18]; only  
91 a limited amount of molecular data has been published so far on the other nacre-bearing  
92 bivalve groups [21-23]. To complete this patchy picture, we have developed a proteomic  
93 investigation on two nacreous bivalves that belong to the Palaeoheterodonta class, and to the  
94 Unionoida order, *Elliptio complanata* and *Villosa lienosa* [24]. Our molecular investigations  
95 are supported by the newly available large transcriptomic databases constructed in parallel  
96 from the two studied species [25-26], and are then providing strong support for the  
97 identification of SMP set of unionoid nacre. The present investigation gives us the  
98 opportunity to determine if bivalve nacles are made by molecular events that are controlled  
99 and conserved by the evolution processes, since the Phanerozoic times.

100 Our high-throughput high-output shotgun approach has allowed us to identify 48 different  
101 proteins from the nacre insoluble matrices, from which 31 are common to the two models.  
102 While recent data suggest a rapid evolution of shell matrix proteins leading to their extreme  
103 diversity [20], our work emphasizes on the contrary a deeply conserved biomineralization  
104 toolkit within nacre-bearing bivalves.

105

106

## 107 **2. Results and Discussion**

108 (a) Protein composition of unionoid nacre matrices

109 In order to investigate the nacre protein set in both *Elliptio complanata* and *Villosa lienosa*,  
110 two closely related freshwater bivalves (Unionoida; Unionidae), the non-fractionated  
111 insoluble matrices derived from respective shell nacre powder were analysed using a XL  
112 Orbitrap nanoLC-MS/MS, after digestion with trypsin enzyme (Figure S1). For both samples,  
113 the peak list generated from the MS/MS spectra was directly interrogated against the  
114 unionoids EST database, comprising 195,192 nucleotide sequences using MASCOT  
115 proteomic search engine (Version 2.1). Using this approach, we were able to enumerate 48  
116 different proteins from the two nacre matrices (Figure 1; Supplementary table S1). More than  
117 80% of these proteins (40 on the 48 identified in total) have been identified with high  
118 confidence, because they are present in both species or are identified by more than one  
119 peptide. Interestingly, 31 of the identified proteins have been detected in both *E. complanata*  
120 and *V. lienosa* testifying of the similarities of the nacre matrix compositions of these two  
121 species. We noticed that all conceptually-translated expressed sequence tag (EST) sequences  
122 that match to the MS/MS peptides present a signal peptide, when sequence exhibits complete  
123 N-terminus, suggesting that these proteins are all secreted by the mantle epithelia through  
124 classical cellular secretion pathway. This list of nacre proteins represents among the largest of  
125 nacre SMP sets described so far, comparable to published SMP set from *Pinctada* and *Mytilus*  
126 models, which count 35 and 42 proteins, respectively [16-18]. While the present results  
127 confirm the presence of previously described protein domains such as Pif, CA, Kunitz-like,  
128 WAP, M-rich, Q-rich, A-rich, or chitin-binding domains [21;23-24], in unionoid shell nacre  
129 matrix, they also contribute to consistently extend the list of proteins associated to nacre  
130 microstructure.

131  
132 The proteomic analysis of these two unionoid nacre matrices reveals a diversity of SMP  
133 structures that can be broadly categorized into 5 main protein groups: ECM (ExtraCellular  
134 Matrix), RLCD-containing (Repetitive-Low Complexity Domain), enzyme, immunity-related,  
135 and 'uncharacterized'. Although our protein list may not be exhaustive - *i.e.* other minor  
136 protein matrix components remain to be characterized - we assume that it contains most of the  
137 abundant nacre SMPs: our approach indeed can identify most of the analogs/homologs of the  
138 main nacre SMP described in pteriomorphid models (Supplementary table S1). Many of these  
139 proteins, such as Pif, MSI60, CA, shematrin-like, Kunitz-like, LamG, chitin-binding  
140 containing proteins, together with A-, D-, G-, M- and Q-rich proteins, appear to be analogues,  
141 if not true homologs, of proteins previously described from the pearl oyster or the edible

142 mussel nacre matrices, and thus, constitute a remarkable set of deeply-conserved nacre  
143 proteins. Indeed, although only genetic information on the gene synteny would reliably  
144 support an hypothesis of homology relation between two proteins/genes of two organisms, we  
145 assume because of sequence of high sequence identities and also because of the specificity of  
146 some SMP domain architecture, that some of these proteins retrieved in these unionoid  
147 organisms would be true homologs of those observed in the pteriomorphid models.

148

#### 149 (b) Extracellular matrix-related (ECM) proteins

150 Among the different unionoid nacre proteins that exhibits ECM protein signature (comprising  
151 collagen, fibronectin, laminin, chitin-binding and other protein- and polysaccharide-  
152 interacting domains), we identified different Pif-like isoforms, various chitin-binding  
153 containing proteins, a Ca-binding protein, a calcium-dependent (C-type) lectin, a mytilin-3  
154 ortholog, together with previously unreported proteins for nacre such as a collagen-alpha-like,  
155 a MSP130-like, DMP-like, and a ANF\_receptor (Figure 2; Supplementary table S1).

156 *Pif-like and Pif-related proteins.* The unionoid nacre matrix exhibits different forms of Pif-  
157 like proteins. Pif-177 (C7G0B5) was first described in the nacre of the pearl oyster [27], and  
158 homologous forms, BMSP-220 and BMSP-like, were subsequently detected in the shell  
159 matrices of the blue mussel *Mytilus galloprovincialis*, and of the giant limpet *Lottia gigantea*,  
160 respectively [28-29]. We have identified here at least 2 different Pif-like isoforms, called Pif-  
161 like 1 and 2, that exhibit both, from N- to C-terminus, the following succession of domains:  
162 one VWA, three CBD2, one RLCD and one LamG. This domain arrangement is characteristic  
163 of the Pif-177/BMSP-200/BMSP-like family [27-29]. Considering that the protein scores  
164 obtained for the Mascot identification of Pif-like 1 is among the highest obtained here, this  
165 supports the idea that the Pif/BSMP protein members are present in very high amount in the  
166 nacre matrix and that Pif/Pif-like proteins must certainly play a key function in mollusc shell  
167 formation [27-29].

168 Interestingly, three other proteins exhibit a domain organisation that partially resembles that  
169 of Pif-like proteins: UNP-2 (1 VWA, 2 long repeats and 1 LamG domains), UNP-3 (1 VWA,  
170 16 CCP and 3 CBD domains), and UNP-5 (2 CBD2 and 1 LamG domains). Furthermore,  
171 various unionoid nacre proteins, called UNP-1, UNP-4, UNP-5, UNP-6 and UNP-7, bear  
172 characteristic chitin- or polysaccharide-binding domains (CBD2, Chitin\_binding\_3 or lectin  
173 C-type). The presence of these various VWA and chitin-binding domains suggest that these  
174 proteins might participate in structuring the chitin/protein nacre scaffold. In addition, we

175 identified other ECM-related proteins, such as DMP-like, MSP130-like, mytilin3-like, ANF-  
176 receptor containing or Ca-binding proteins, for which homologs have previously been  
177 described from other proteins associated with biomineralizations [30-32]. The involvement of  
178 these proteins in biomineralization processes is discussed below.

179

#### 180 (c) Repeated low-complexity domain (RLCD) containing proteins

181 Our proteomic investigation also highlights the presence of a large set of 16 RLCD-containing  
182 proteins (supplementary table S1) for which similar proteins (that are genuine orthologous for  
183 some of them) were previously observed in *Pinctada* nacre, namely MSI60-like, shematin,  
184 G-, Q-, Y-, D- and M-rich proteins [2]. In addition, we identified new features such as a  
185 byssal protein-like, the homologs of which have been detected some years ago in the byssus  
186 of the blue mussel [33].

187 *MSI60-like*. This protein fragment presents high sequence similarities with MSI60, presenting  
188 characteristic repeats of G-rich and poly-A blocks (45% identity and E-value 3.1E-55), and  
189 initially described as a framework protein in the shell of *Pinctada fucata* [34]. MSI60 is a  
190 nacre-specific insoluble protein that exhibits poly-A and poly-G blocks giving MSI60 a  
191 certain similarity with hydrophobic spider and worm silk fibroins. More recently, another  
192 protein (has\_CL10Contig2) with global similarities but no direct homology to MSI60  
193 sequence has also been identified in the shell nacre of the abalone *Haliotis asinina* [19]. This  
194 suggests once more that such G- and A-rich proteins with hydrophobic silk-fibroin-like  
195 domains are key-players in nacre formation, in both bivalves and gastropods.

196 *Shematin-like*. Only one protein corresponding to a shematin-like protein has been identified  
197 in the two unionoids according to one peptide that gives a heterologous match with the EST  
198 sequence UTP\_var00312 available from the brook floater *Alasmidonta vericosa*, another  
199 unionoid bivalve. This protein presents strong sequence similarity (72% identity and E-value  
200 5E-155) with silkmapiin a nacre protein from the unionoid *Hyriopsis cumingii* [35], that  
201 present sequence similarity with shematin proteins previously retrieved from *Pinctada* shell.  
202 The overall primary structure of shematrins is characterized by a signal peptide, G-G-Y-repeat  
203 motif, together with other more variable G- and Y-rich repeated low-complexity domains  
204 (RLCDs) and KKKY N-termini [36], that are also observed in this novel unionoid putative  
205 member. Shematin-likes constitute one of the main SMP family, found in both nacre and  
206 prismatic layer of the shell of *Pinctada spp.*, and their corresponding transcripts are highly  
207 expressed in the mantle [2;20]. Surprisingly, their homologous sequences lack in the TSA

208 databases of *E. complanata* and *V. lienosa*. We assume that the matching peptide observed in  
209 the two unionoid models may correspond to a genuine shematrin-like protein, similar to the  
210 one derived from *A. vericosa* EST. The apparent absence of shematrin-like transcripts in the  
211 *E. complanata* and *V. lienosa* databases call for explanations at two levels: a) Restricted  
212 temporal expression [37], outside the 'window' of tissue sampling. Indeed, previous  
213 investigations have highlighted that key SMPs could be underrepresented or absent from a  
214 mantle EST database for such a reason [29]. b) Spatial expression of the shematrin transcripts  
215 restricted to the mantle; their absence in the transcriptomes of *E. complanata* and *V. lienosa*  
216 may be simply due to tissue sampling for EST construction, which was not particularly  
217 focused on the mantle [25;26].

218

219 *Byssal protein-like, N-, T-, Q-, G- and M-rich proteins.*

220 Our proteomic investigation has detected in the shell nacre of *V. lienosa* a sequence, which  
221 exhibits global similarities with a byssal protein-like from the mussel *Mytilus*  
222 *galloprovincialis* (33% identity). This protein exhibits repeat domains that are enriched in G,  
223 D, N and Y residues (Supplementary figure S2; supplementary table S1). Byssus is a silk-like  
224 acellular thread that is secreted by the foot of various bivalves, and that firmly anchors the  
225 organism to its substratum owing to strong adhesive distal plaques. A very recent proteomic  
226 investigation [38] has shown that several proteins constituting the byssal acellular structures  
227 (tyrosinase, A2M, EGF and VWA containing proteins) are common with those of the shell  
228 layers, claiming for similarities of the formation and the evolution of these two structures.

229 In addition, mollusc matrix proteins rich in Q have also been found in bivalves: for example  
230 MPN88 was previously characterized from the pearl oyster *Pinctada margaritifera* [39]. In  
231 the shell of the gastropod *Lottia*, at least 4 different matrix proteins present similar features  
232 [29]. Interestingly, vertebrate teeth contain various Q-rich proteins belonging to the secreted  
233 calcium-binding phosphoprotein family, which are believed to interact with calcium ions and  
234 regulate the tooth mineralization process [40]. In parallel, it has been proposed that the  
235 numerous Q residues of various silk-like fibroins, which also present numerous A- and G-rich  
236 domains, are implicated in the tensile mechanical properties of these proteins [41]. Few  
237 proteins with M- and G-rich composition were identified among the RLCD-containing shell  
238 proteins listed in this study. Proteins with similar enrichments in M and G residues have also  
239 been recently described in the matrix of *Pinctada* [42], of *Haliotis* [19] and of *Lottia* [29].

240 However, the functional characterization of these characteristic domains in mollusc SMPs  
241 remains to be done.

242 In the present case, in spite of overall sequence similarities observed within these several  
243 RLCD protein categories identified in different models, it remains difficult to clearly outline  
244 whether they are truly homolog considering limitation of standard Blastp tools for low-  
245 complexity sequences, the fast rate of evolution of these domains [41;43] and that fortuitous  
246 low-complexity sequence similarities can be obtained between non-homologous SMPs that  
247 have evolved completely independently.

248

#### 249 (d) Other bivalve shell-conserved proteins

250 *Carbonic anhydrase*. Carbonic anhydrase (CA) is also a ubiquitous enzyme that is essential  
251 for calcium carbonate biomineral formation. It has been found in the organic matrices of  
252 various metazoan skeletons [44-46]. In molluscs, shell-specific form of CA, exhibiting G, N  
253 and D-rich LCDs, have been isolated first from the shell matrix of the pearl oysters *Pinctada*  
254 sp. [15]. In our study, the CAs detected in the two unionoid naces do not possess similar  
255 supernumerary RLC domains, suggesting that matrix-associated CAs do not necessarily  
256 require such domains for being occluded in calcium carbonate microstructure or for exhibiting  
257 affinity with calcium carbonate mineral surfaces. At last, our results confirm the presence of  
258 CA in a non-pteriomorph bivalve shell as previously suggested [21;23]. Taken together, our  
259 findings reemphasize the central role played by extracellular CAs in CaCO<sub>3</sub> biomineralization  
260 processes.

261 *Chitin-interacting enzymes*. Among the SMPs, we identified two enzymes, namely chitinase 3  
262 and chitobiase, which both exhibit glyco\_hydro\_18 and glyco\_hydro\_20 domains. These  
263 domains belong to the glycoside hydrolases family that hydrolyses the glycosidic bond  
264 between carbohydrates or between a carbohydrate and other components. Indeed, chitin is  
265 known to represent a major polysaccharide in mollusc shells. It is involved in constituting a 3-  
266 dimensional framework, in association with silk-like and acidic proteins in which nacre tablet  
267 crystals grow [10]. The identification of chitin-interacting enzymes, coupled with the  
268 detection of several chitin-binding domains in bivalve nacre SMPs strongly suggests an  
269 important role of chitin-cleaving enzymes in the fine molecular rearrangement of the chitin  
270 framework following the secretion of the nacre macromolecular ingredients at the vicinity of  
271 nascent growing mineral tablets.

272 *Tyrosinase*. The first mention of the involvement of a tyrosinase in bivalve shell formation

273 concerned the deposition of the periostracum and of the prismatic layer in the pearl oyster  
274 [47] In particular, it was shown by *in situ* hybridization that the zone of the highest expression  
275 of tyrosinase was the mantle edge from which these two layers are secreted. Recently, this  
276 enzyme has also been detected in lesser amount in nacre shell structure [16]. Tyrosinase is an  
277 oxidase that controls the production of protein melanogenesis *via* cross-linking by  
278 hydroxylation of the phenol groups present in tyrosine residues and their conversion to  
279 quinones. Biomineral-associated tyrosinases contribute to periostracum tanning [47]. They  
280 may be also involved in the maturation and hardening of the biomineral-hydrogel (that  
281 precedes crystallization) in prismatic as well as in nacreous shell layers [10].

282 *Thioredoxin (TRX) and superoxide dismutase (SOD)*. Two enzymes involved in antioxidant  
283 processes, TRX and SOD, were also detected in the shell nacre of *V. lienosa*. Besides the  
284 identification of various isoforms of peroxidases in *Lottia* shell matrix [29], there are to date  
285 only a couple of examples of such redox enzymes in mollusc shell matrices [17;48]. In the  
286 present study, TRX and SOD were detected only via a limited number of peptides, suggesting  
287 that they may be minor component of the nacre matrix. Their putative function in shell  
288 biomineralization remains enigmatic. We cannot exclude the possibility that they are  
289 contaminants: SOD, for example, constitutes the main hemolymph protein, in charge of  
290 oxygen transport in bivalves [49]; its accidental occlusion in shell calcified tissues is not an  
291 unlikely scenario.

292 *Immunity-related proteins*. Finally, we detected, in both *Elliptio* and *Villosa*'s nacre matrices,  
293 four proteins with potential immunity-related functions. They exhibit indeed Kunitz-like  
294 (KU), or whey acidic protein (WAP) or macroglobulin protease inhibitor domains (Figure 1;  
295 supplementary table S1). The presence of such protease inhibitors in an acellular biomineral  
296 is, at first sight, puzzling. However our finding does not constitute a single observation, since  
297 the presence of such immunity-associated domains in shell proteins has been already noticed  
298 in different metazoan calcium carbonate biominerals: the shells of abalones [19;50], of pearl  
299 oysters [2;51-52], of the giant limpet [29] and, at last, the chicken egg shells [46]. One has  
300 proposed that these molecules are involved either in immunological defence mechanisms, or  
301 in the regulation of the matrix maturation, by controlling cleavage processes of other matrix  
302 proteins [53-54].

303

304 (e) Inherited set of nacre and shell matrix proteins in bivalves

305 One of the most striking results of our study was the detection, in *Elliptio and Villosa's* shell  
306 matrices, of various proteins that exhibit high sequence homologies with SMPs extracted from  
307 the nacreous shell layers of *Pinctada* and/or *Mytilus* bivalves. This constitutes a very  
308 consistent evidence of the existence of a set of ancient, *i.e.* Palaeozoic, nacre proteins shared  
309 between the various nacre-forming bivalve taxa (Figure 3).

310 More than two decades ago, when molluscan nacre matrices were solely analyzed for their  
311 amino acid compositions after hydrolysis of the bulk, the similarity of their compositions  
312 characteristically marked by high contents in glycine, alanine and aspartate residues,  
313 suggested identical molecular mechanisms for controlling the deposition of nacre tablets in  
314 the different nacre-bearing molluscs [55]. But, since the publication of the first full primary  
315 structure of a nacre protein, in 1996 [15], the increasing number of discovered SMPs has point  
316 out an extraordinary diversity of nacre-associated proteins among the different taxa [8;9]. This  
317 suggested on the contrary the use of different protein toolkits for nacre deposition. This view  
318 seemed to prevail, in particular with the finding that the bivalve *Pinctada* and the gastropod  
319 *Haliotis* possess absolutely dissimilar sets of shell-building genes [19;20]. This abrupt  
320 conclusion was however counterbalanced later by one of our studies that clearly demonstrated  
321 that the nacre of the edible mussel *Mytilus* and the non-nacreous shell microstructure of the  
322 limpet *Lottia*, contains number of proteins that are similar - if not homologous - to that of  
323 *Pinctada's* nacre [2;29;30]. The present set of data supports and reinforces the "deep origin  
324 scenario" by revealing a shared protein toolkit in the nacre of bivalve species that belong to  
325 three clades, Mytiloidea, Pterioidea (both belonging to Pteriomorphia subclass) and Unionoidea  
326 (the main order of the Palaeoheterodonta subclass) that diverged in the Palaeozoic times [56].  
327 The list of shared nacre proteins between the three main bivalve models comprises: MSI60,  
328 Pif, CA, macroglobulin, VWA-, LamG-, CBD2- and Kunitz-like-containing proteins, along  
329 with various RLCD protein exhibiting A-, D-, G-, Q- and M-rich domains. This short list  
330 potentially represents the inherited ancestral toolkit - or at least a part of it - required for nacre  
331 formation. Other proteins appear to be shared by only two species out of three, and are  
332 probably related with taxon specificity adaptations. One has to notice that some of the  
333 proteins listed on figure 3 have been also identified in the prismatic layers of the three  
334 bivalves, suggesting that their molecular functions might not be exclusively restricted to nacre  
335 deposition.

336 By identifying nacre proteins from two non-pteriomorph species and reporting a deeply  
337 conserved nacre protein set in bivalves this work adds new evidence that that the calcifying

338 matrix of molluscs is comprised of both deep conservations and lineage-specific protein  
339 novelties. The comparison of these bivalve-conserved protein sets to those previously  
340 detected in gastropod nacre is confirming the global dissimilarity of the nacre SMP sets of  
341 bivalves and of gastropods (at least those of the abalone) [19]. Bivalve and gastropod exhibit  
342 different kinds of nacles (respectively, sheet and columnar nacles), which homology still  
343 constitute an actual debate that still oppose parcimony principles [14], crystallographic and  
344 microstructural textures [11;57], along with paleontological and molecular evidences  
345 [12;13;20].

346  
347 Figure 4 summarizes all available information on the occurrence of protein domains observed  
348 from shell proteome of various mollusc models, comprising nacre and prismatic shell layers  
349 of bivalves (*Unionoids*, *Pinctada* and *Mytilus*), cross-lamellar layers of gastropod (*Lottia* and  
350 *Cepaea*), and finally, fibrous layers of brachiopods, taken as an outgroup. This figure shows  
351 that several proteinaceous domains, which appear to be shared between the different nacre  
352 models, are also detected in bivalve prismatic layers or in the shell of cross-lamellar  
353 gastropods. This clearly suggests that these domains are not specifically involved in nacre  
354 formation, but that they display general function in shell formation.

355 The brachiopod shell proteomes, retrieved from the CaCO<sub>3</sub> shell of *Magellania venosa* [58]  
356 and the CaPO<sub>3</sub> one of *Lingula anatina* [59], respectively, exhibit many similarities with those  
357 of molluscs in their respective protein and functional domain compositions. The list of shared  
358 domains comprises potentially key contributors of shell formation processes, such as D-, A-  
359 and G-rich, VWA, EGF, CCP, peroxidase, tyrosinase, chitinase, CA, KU, A2M and CBD2.  
360 Furthermore, Luo and co-workers [59] notice also that genes shared between *Lingula* and  
361 molluscs, such as calcium-dependent protein kinase and chitin synthase, exhibit high  
362 expression in larvae and mantle, indicating that they may also be involved in brachiopod shell  
363 formation. Taken together, these results indicate that a conserved molecular machinery exists  
364 for shell biomineralization in brachiopods and molluscs. This assumption needs however a  
365 further validation via functional analyses.

366

367 (h) Are metazoan SMPs deeply conserved?

368 The appealing scenario of an ancient and common origin of the biomineralization within the  
369 metazoan has been proposed at various occasions [3;60]. This scenario is based on the  
370 supposed existence of a shared ancestral metazoan toolkit that was implemented before the

371 main metazoan radiations. But to date, the data that support this view still remain extremely  
372 tenuous. For example, no one ever evidenced a universal molecular marker of the skeletal  
373 matrices of all calcifying metazoans. Many skeletal matrix proteins belong to families that are  
374 not necessarily specific of biomineralization processes, suggesting that many proteins could  
375 have been coopted secondarily for calcification purpose. For example, although CA has been  
376 observed in various biomineralization models, comprising egg-shell, echinoderm skeleton,  
377 mollusc shell or sponge spicules, it constitutes a broad and ubiquitous protein family  
378 presenting various members in all organisms, calcifying or not; their phylogenetic analysis  
379 shows a very complex evolutionary history, indicating that they could have been recruited  
380 several times, in independent manners, in biomineralization structure within the different  
381 metazoan clades [61].

382 At the opposite of the CA example, MSP-130 represents a remarkable illustration of a  
383 conserved molecular function that may be strictly restricted to biocalcification, but present in  
384 distinct metazoan lineages. MSP-130 is a protein, initially identified in the sea urchin  
385 *Strongylocentrotus purpuratus* [62], which expression is specific to primary mesenchyme  
386 cells [63] - the cells that initiate the skeletal tissues in echinoderms - and that represents one  
387 of the main constituent of the calcifying matrix of the different skeletal structures, including  
388 the teeth, the spicules, the test or the spines [64]. So far, no other function than those related  
389 to biomineralization has been described for this protein. Interestingly, during our previous  
390 investigation of the shell proteins of the Pacific oyster *Crassostrea gigas*, we detected a  
391 protein, called gigasin-3, which partial sequence exhibits noticeable similarity with *S.*  
392 *purpuratus* MSP-130 [31]. Even more recently, the *msp130* gene was also identified in a  
393 calcified tube-forming polychaete [65]. With the present study, the recognition in nacre  
394 matrix of two unionoids of a similar MSP-130-like protein firmly supports the idea that this  
395 biomineralization-specific protein or protein family is shared between different metazoan  
396 calcifying lineages, reintroducing the scenario of common ancestral mechanism for metazoan  
397 biomineralization processes.

398 In addition, we have detected that the two unionoid proteomes contain both a dentin-matrix  
399 protein-like (DMP-like), exhibiting a remarkable FAM20C domain (Supplementary figure  
400 S3). Indeed, FAM20C is a kinase that phosphorylates the majority of the phosphoproteome in  
401 the extracellular matrices of bones and teeth, constituting a key player of vertebrate  
402 biomineralization process [66]. Other recent investigations have revealed the presence of  
403 FAM20C containing protein in the shell matrix of the giant limpet *Lottia gigantea* [48], and

404 of the brachiopod *Magellania venosa* [58]. The presence of such key-protein, regulating the  
405 biomineralization formation of vertebrates, in the shell matrices of molluscs and brachiopods  
406 strongly reinforces the idea of common molecular machinery, supporting the scenario of a  
407 conserved biomineralization toolkit between different metazoan lineages.

408

409

### 410 **3. Conclusion**

411 Our study presents proteomic results obtained from the nacre matrices of two unionoid  
412 (Paleoheterodonta) bivalves. Our approach is robust and powerful since it allows annotating  
413 genes encoding proteins that are undoubtedly shell matrix constituents, therefore, putatively  
414 important players in the nacre assembling process. It excludes genes that encode mantle-  
415 secreted proteins – recognizable by their signal peptide signature – but which are not occluded  
416 within the calcified tissue, *i.e.* proteins, which are not constituents of the shell organic matrix.  
417 We are fully conscious that some of these proteins, not detected by our approach, may be  
418 important players for calcification as well [67].

419 Our study has macro-evolutionary implications. Nacre is supposed to represent an ancestral  
420 shell microstructure, shared by different orders within the bivalve class. Because it remained  
421 almost unchanged until now, from a microstructural viewpoint, this suggests that at least a  
422 part of the molecular toolkit used for constructing nacre must have been kept conserved  
423 within these nacre-forming clades. Our proteomic approach focused on the unionoid bivalves  
424 has allowed detecting several genuine sequence homologies with known sequences of nacre  
425 proteins of pteriomorph bivalves, but also with other SMPs from gastropod and brachiopod  
426 models, unveiling a part of a deeply conserved shared legacy.

427

428

### 429 **4. Material and methods**

#### 430 (a) Nacre matrix extraction

431 Fresh *Villosa lienosa* (6-8 cm in length) and *Elliptio complanata* (8-10 cm in length) shells  
432 were collected from Chewacla Creek near Auburn, Alabama (USA), in April 2012, and from  
433 Cree Lake near Cochrane, Ontario (Canada), in spring 2011, respectively. Among the  
434 paleoheterodont bivalves, both are representatives of unionoid order, the shell microstructures  
435 of which are characterized by the association of aragonitic prisms and nacre. Superficial  
436 organic contaminants as well as the periostracum were removed by incubating intact shells in

437 NaOCl (5%, v/v) for 24-48 h [68]. Shells were then thoroughly rinsed with water. The  
438 external prismatic layer was mechanically removed and the shell nacre broken into 1-mm  
439 large fragments before being ground to fine powder ( $> 200 \mu\text{m}$ ) that was subsequently  
440 decalcified in cold acetic acid overnight (10%; 4 °C). The insoluble nacre matrix was then  
441 collected by centrifugation (15,000 g; 10 min; 4 °C), and the pellet rinsed six times with  
442 MilliQ water by series of resuspension-centrifugation before being freeze-dried and weighed.

443

#### 444 (b) Peptide digest proteomic analyses

445 In-solution digestions of insoluble nacre matrix samples were performed. One mg of the  
446 matrices was reduced with 100  $\mu\text{L}$  of 10 mM dithiothreitol (Sigma-Aldrich, France) in 500  
447 mM triethylammonium bicarbonate pH 8.0 for 30 min at 57° C. Fifteen  $\mu\text{L}$  of iodoacetamine  
448 (50 mM, final concentration) was added and alkylation was performed for 30 min at room  
449 temperature in the dark, then digestion was performed by adding 10  $\mu\text{g}$  of trypsin (T6567,  
450 proteomics grade, Sigma). The samples were incubated overnight at 37 °C, then centrifuged  
451 (30 min, 14,000 g) and 5  $\mu\text{L}$  of the acidified supernatants was injected into the tandem mass  
452 spectrometer with an electrospray source coupled to a liquid chromatography system analysis  
453 (nanoLC-ESI-MS/MS). The protein digest concentration was prior estimated using a micro-  
454 BCA kit (Sigma-Aldrich, USA), with BSA as protein standard.

455 Protein digests were analyzed using a nano-LC (Ultimate 3000, Dionex) coupled to an ESI-  
456 LTQ-Orbitrap (LTQ Orbitrap XL, Thermo Scientific) mass spectrometer [69]. Above 10  $\mu\text{g}$   
457 of AIM digest protein digests solubilized in 10% ACN with 0.1% formic acid were injected in  
458 triplicates by the autosampler and concentrated on a trapping column (Pepmap, C<sub>18</sub>, 300  $\mu\text{m}$  x  
459 5 mm, 5  $\mu\text{m}$  100 Å, Dionex) with water containing 10% ACN with 0.1% formic acid (solvent  
460 A). After 5 min, the peptides eluted onto a separation column (Pepmap, C<sub>18</sub>, 75  $\mu\text{m}$  x 500  
461 mm, 2  $\mu\text{m}$  100 Å, Dionex) equilibrated with solvent A. Peptides were separated with a 2h-  
462 linear gradient of 80% ACN + 0.1% formic acid (solvent B) at flow rate of 200 nL.min<sup>-1</sup>. The  
463 LTQ-Orbitrap mass spectrometer is outfitted with a nano-ESI electrospray source. Spectra of  
464 multiple charged precursor ions (+2 to +4) were collected from  $m/z$  300-2000 at a resolution  
465 of 30,000 in the profile mode followed by data dependent CID and/or HCD spectra of the ten  
466 most intense ions. A dynamic exclusion window of 60 s was used to discriminate against  
467 previously analyzed ions.

468

#### 469 (c) Bioinformatics

470 The MS/MS data were used for database searches using an in house version of the MASCOT  
471 search engine (Matrix Science, London, UK; version 2.1) against 138,345 and 46,051 TSA  
472 nucleotide sequences derived from *E. complanata* and *V. lienosa* EST libraries [25;26],  
473 respectively (plus few hundreds *Alasmidonta* spp. sequences), downloaded in December 2015  
474 from the NCBI server (<http://www.ncbi.nlm.nih.gov>). LC-MS/MS data generated by each  
475 shell sample and protein band were searched separately, using carbamido-methylation as a  
476 fixed modification and methionine oxidation as variable modification. The peptide MS  
477 tolerance was set to 10 ppm and the MS/MS tolerance was set to 20 mDa. Proteins with at  
478 least two different peptides or identified in both species were considered to be fully valid.  
479 Protein identification was performed using BLAST searches against the UniProtKB/Swiss-  
480 Prot protein sequence database ([www.uniprot.org](http://www.uniprot.org)), retrieving only hit with e-value < 7E-8,  
481 and without filtering low complexity region. Signal peptides were predicted using SignalP 4.0  
482 (<http://www.cbs.dtu.dk/services/SignalP>) and conserved domains from database models were  
483 predicted using external source database SMART (<http://smart.embl-heidelberg.de>). 3-D  
484 protein structures were predicted according to sequence homologies using the Phyre 2.0  
485 online tool (<http://www.sbg.bio.ic.ac.uk/phyre2>) [70].

486  
487

488 **Data accessibility.** Supplementary table S1 containing the complete list and description of all  
489 proteins identified in *E. complanata* and *V. Lienosa* nacre matrices by shotgun proteomics has  
490 been uploaded as electronic supplementary materials.

491

492 **Abbreviations:** A2M, alpha-2 macroglobulin; APase, alkaline phosphatase; ANF,  
493 extracellular ligand binding; BMSP, blue mussel shell protein; C1q, complement complex  
494 protein 1; CA, carbonic anhydrase; CBD, peritrophin-A chitin-binding domain; CCP/SUSHI,  
495 complement control protein; Chit\_bind, chitin-binding domains; CLECT, C-type lectin;  
496 Copamox, copper amine oxidase; DMP, dentin matrix protein; EGF, epidermal growth factor;  
497 FAM20C, family with sequence similarity 20 - member C; FN3, fibronectin 3; IGF-BP,  
498 insulin growth factor-binding protein; KU, Kunitz-like domain; LamG, laminin G; MSP,  
499 mesenchym-specific protein; MSI60, matrix silk-like insoluble protein 60; PIF/Pif177,  
500 *Pinctada fucata* 177-kDa protein, RLCD, repetitive low-complexity domain; SMP, shell  
501 matrix protein; SCP, Cysteine-rich secretory protein; SOD, superoxide dismutase; TIMP,  
502 tissue inhibitor of metalloprotease; TRX, thioredoxin; UNP, uncharacterized nacre protein;  
503 VWA, von Willebrand factor type A; WAP, whey acidic protein; ZP, zona pellucida.

504

505 **Author's contribution.** B.M., G.B., S.B. & F.M. conception, design and coordination; J.A.,  
506 A.M., L.M. preparation of the sample, analysis and interpretation of the data. All author  
507 contribute to the preparation and the revision of the manuscript.

508

509 **Competing interests.** The authors have no competing financial interests.

510

511 **Funding.** Jaison Arivalagan is supported by a funding from the Marie Curie European Union  
512 Seventh Framework Programme under grant agreement no. 605051.

513

514 **Acknowledgments.** We are especially grateful to Dr. James Stoeckel and Dr. Emily Awad for  
515 kindly providing us the *Villosa lienosa* and *Elliptio complanata* shells.

516

517

## 518 **References**

519 [1] Taylor J, Kennedy WJ, Hall A. 1973 The shell structure and mineralogy of the Bivalvia,  
520 Part II, Lucinacea–Clavagellacea. *Bull Brit Mus Zool* **22**, 253–294.

521 [2] Marie B, Joubert C, Tayale A, Zanella-Cléon I, Belliard C, Cochenec-Loreau N,  
522 Piquemal D, Marin F, Gueguen Y, Montagnani C. 2012 Different secretory repertoires  
523 control the biomineralization processes of prism and nacre deposition of the pearl oyster  
524 shell. *Proc Natl Acad Sci* **109**, 20986-20991.

525 [3] Lowenstam HA, S. Weiner S. 1989 On Biomineralization. Oxford University Press, New  
526 York.

527 [4] Suzuki M, Nagasawa H. 2013 Mollusk shell structures and their formation mechanism.  
528 *Can J Zool* **91**, 349-366.

529 [5] Mann S. 2001 Biomineralization: Principles and Concepts, in *Bioinorganic Materials*  
530 *Chemistry*. Oxford University Press, New York.

531 [6] Falini G, Albeck S, Weiner S, Addadi L. 1996 Control of aragonite and calcite  
532 polymorphism by mollusk shell macromolecules. *Science* **271**, 67–69.

533 [7] Berland S, Delattre O, Borzeix S, Catonne Y, Lopez E. 2005 Nacre/bone interface changes  
534 in durable nacre endosseous implants in sheep. *Biomaterials* **26**, 2767-2773.

535 [8] Marin F, Luquet G, Marie B, Medakovic D. 2008 Molluscan shell proteins: primary  
536 structure, origin, and evolution. *Curr Top Dev Biol* **80**, 209–276.

- 537 [9] Marin F, Le Roy N, Marie B. 2012 The formation and mineralization of mollusc shell.  
538 *Front Biosci* **4**, 1099–1125.
- 539 [10] Addadi L, Joester D, Nudelman F, Weiner S. 2006 Mollusk shell formation: a source of  
540 new concepts for understanding biomineralization processes. *Chem Rev* **12**, 980–987.
- 541 [11] Checa A, Rodriguez-Navarro A. 2001 Geometrical and crystallographic constrains  
542 determine the self-organisation of the shell microstructures in Unionidae (Bivalvia:  
543 Mollusca). *Proc Biol Sci* **268**, 771-778.
- 544 [12] Kouchinsky A. 2000 Shell microstructures in Early Cambrian molluscs. *Acta Palaeontol*  
545 *Pol* **45**, 119–150.
- 546 [13] Vendrasco MJ, Porter SM, Kouchinsky A, Li G, Fernandez CZ. 2010 New data on  
547 molluscs and their shell microstructures from the Middle Cambrian Gowers Formation,  
548 Australia. *Palaeontology* **53**, 97–135.
- 549 [14] Carter JG. 1990 Skeletal Biomineralization: Patterns, Processes and Evolutionary Trends.  
550 Van Nostrand Reinhold, New York.
- 551 [15] Miyamoto H, Miyashita T, Okushima M, Nakano S, Morita T, Matsushiro A. 1996 A  
552 carbonic anhydrase from the nacreous layer in oyster pearls. *Proc Natl Acad Sci* **93**, 9657–  
553 9660.
- 554 [16] Liu C, Li S, Kong J, Liu Y, Wang T, Xie L, Zhang R. 2015 In-depth proteomic analysis  
555 of shell proteins of *Pinctada fucata*. *Sci Rep* **5**, 17269.
- 556 [17] Gao P, Liao Z, Wang X, Bao L, Fan M, Li X, Wu C, Xia S. 2015 Layer-by-layer  
557 proteomic analysis of *Mytilus galloprovincialis* shell. *PLoS ONE* **10**:e0133913.
- 558 [18] Liao Z, Bao L, Fan M, Gao P, Wang X, Qin C, Li X. 2015 In-depth proteomic analysis  
559 of nacre, prism, and myostracum of *Mytilus* shell. *J Proteomics* **122**, 26-40.
- 560 [19] Marie B, Marie A, Jackson DJ, Dubost L, Degnan BM, Milet C, Marin F. 2010  
561 Proteomic analysis of the organic matrix of the abalone *Haliotis asinina* calcified shell.  
562 *Proteome Sci* **8**, 54.
- 563 [20] Jackson DJ, McDougall C, Woodcroft B, Moase P, Rose RA, Kube M, Reinhardt R,  
564 Rokshar DS, Montagnani C, Joubert C, Piquemal D, Degnan BM. 2010 Parallel evolution  
565 of nacre building gene sets in molluscs. *Mol Biol Evol* **27**, 591-608.
- 566 [21] Marie B, Zanella-Cléon I, Le Roy N, Becchi M, Luquet G, Marin F. 2010 Proteomic  
567 analysis of the acid-soluble nacre matrix of the bivalve *Unio pictorum*: detection of novel  
568 carbonic anhydrase and putative protease inhibitor proteins. *ChemBioChem* **11**, 2138-2147.
- 569 [22] Ramos-Silva P, Benhamada S, Le Roy N, Marie B, Guichard N, Zanella-Cléon I,

- 570 Plasseraud L, Corneillat M, Alcaraz G, Kaandorp J, Marin F. 2012 Novel molluscan  
571 biomineralization proteins retrieved from proteomics: a case study with Upsalin.  
572 *Chembiochem* **13**, 1067-1078.
- 573 [23] Berland S, Ma Y, Marie A, Andrieu J-P, Bédouet L, Feng Q. 2013 Proteomic and profile  
574 analysis of the proteins laced with aragonite and vaterite mussel *Hyriopsis cumingii* shell  
575 biominerals. *Prot Peptide letters* **20**, 1170-1180.
- 576 [24] Marie B, Aviralagan J, Dubost L, Berland S, Marie A, Marin F. 2015 Unveiling the  
577 evolution of bivalve nacre proteins by shell proteomics of Unionoids. *Key Eng Mater* **672**,  
578 158-167.
- 579 [25] Wang R, Li C, Stoeckel J, Moyer G, Liu Z, Peatman E. 2012 Rapid development of  
580 molecular resources for a freshwater mussel, *Villosa lienosa* (Bivalvia: Unionidae), using  
581 an RNA-seq-based approach. *Freshw Sci* **31**, 695–708.
- 582 [26] Cornman RS, Robertson LS, Galbraith H, Blakeslee C. 2014 Transcriptomic analysis of  
583 the mussel *Elliptio complanata* identifies candidate stress-response genes and an  
584 abundance of novel or noncoding transcripts. *PLoS One* **9**:e112420.
- 585 [27] Suzuki M, Saruwatari K, Kogure T, Yamamoto Y, Nishimura T, Kato T, Nagasawa H.  
586 2009 An acidic matrix protein, Pif, is a key macromolecule for nacre formation. *Science*  
587 **325**, 1388–90.
- 588 [28] Suzuki M, Iwasima A, Tsutsui N, Ohira T, Kogure T, Nagasawa H. 2011 Identification  
589 and characterisation of a calcium carbonate-binding protein, blue mussel shell protein  
590 (BMSP), from the nacreous layer. *ChemBioChem* **16**, 278–287.
- 591 [29] Marie B, Jackson DJ, Ramos-Silva P, Zanella-Cléon I, Guichard N, Marin F. 2013 The  
592 shell-forming proteome of *Lottia gigantea* reveals both deep conservations and lineage-  
593 specific novelties. *FEBS J* **280**, 214-232.
- 594 [30] Marie B, Le Roy N, Zanella-Cléon I, Becchi M, Marin F. 2011 Molecular evolution of  
595 mollusc shell proteins: insights from proteomic analysis of the edible mussel *Mytilus*. *J*  
596 *Mol Evol* **72**, 531–546.
- 597 [31] Marie B, Zanella-Cléon I, Guicahrd N, Becchi M, Marin F. 2011 The calcifying shell  
598 matrix of the Pacific oyster *Crassostrea gigas*: proteomic identification of novel proteins.  
599 *Mar. Biotechnol* **13**,1159-1168.
- 600 [32] Xiao J, Tagliabracci V, Wen J, Kim S, Dixon J. 2013 Crystal structure of the Golgi  
601 casein kinase. *Proc Natl Acad Sci* **110**, 10574-10579.
- 602 [33] Sagert J, Waite J. 2009 Hyperunstable matrix protein in the byssus of *Mytilus*

- 603 *galloprovincialis*. *J Exp Biol* **212**, 224-2236.
- 604 [34] Sudo S, Fujikawa T, Nagakura T, Ohkubo T, Sakagushi K, Tanaka M, Nakashima K,  
605 Takahashi T. 1997 Structures of mollusc shell framework proteins. *Nature* **387**, 563–564.
- 606 [35] Liu X, Dong S, Jin C, Bai Z, Wang G, Li J. 2015 Silkmapin of *Hyriopsis cumingii*, a  
607 novel silk-like shell matrix protein involved in nacre formation. *Gene* **555**, 217-222.
- 608 [36] Yano N, Nagai K, Morimoto K, Miyamoto H. 2006 Shematrix: a family of glycine-rich  
609 structural proteins in the shell of the pearl oyster. *Comp Biochem Physiol* **144**, 254–262.
- 610 [37] Miyazaki Y, Usui T, Kajikawa A, Hishiyama H, Matsuzawa N, Nishida T, Machii A,  
611 Samata T. 2008 Daily oscillation of gene expression associated with nacreous layer  
612 formation. *Front Mater Sci China* **2**, 162-166.
- 613 [38] Qin CL, Pan QD, Qi Q, Fan MH, Sin JJ, Li NN, Liao Z. 2016 In-depth proteomic  
614 analysis of the byssus from marine mussel *Mytilus coruscus*. *J Proteomics* **144**, 87-98.
- 615 [39] Berland S, Marie A, Duplat D, Milet C, Sire J-Y, Bédouet L. 2011 Coupling proteomics  
616 and transcriptomics for identification of novel variant forms of mollusc shell proteins: a  
617 study with *P. margaritifera*. *ChemBioChem* **12**, 950-961.
- 618 [40] Kawasaki K, Buchanan AV, Weiss KM. 2009 Biomineralization in humans: making the  
619 hard choices in life. *Annu Rev Genet* **43**, 119–142.
- 620 [41] Catesy J, Hayashi C, Motruik D, Woods J, Lewis R. 2001 Conservation and convergence  
621 of spider silk fibroin sequences. *Science* **291**, 2603-2605.
- 622 [42] Marie B, Joubert C, Tayale A, Zanella-Cléon I, Marin F, Gueguen Y, Montagnani C.  
623 2012 MRNP34, a novel methionine-rich protein from the pearl oysters. *Amino Acids* **5**,  
624 2009–2017.
- 625 [43] McDougall C, Aguilera F, Degnan BM. 2013 Rapid evolution of pearl oyster shell matrix  
626 proteins with repetitive, low complexity domains. *J R Soc Interface* **10**, 20130041.
- 627 [44] Tambutté S, Tambutté E, Zoccola D, Caminiti N, Lotto S, Moya A, Allemand D, Adkins  
628 J. 2007 Characterization and role of carbonic anhydrase in the calcification process of the  
629 azooxanthellate coral *Tubastrea aurea*. *Mar Biol* **151**, 71–83.
- 630 [45] Jackson DJ, Macis L, Reitner J, Degnan BM, Wörheide G. 2007 Sponge paleogenomics  
631 reveals an ancient role for carbonic anhydrase in skeletogenesis. *Science* **216**, 1893–1895.
- 632 [46] Mann K, Macek B, Olsen J. 2006 Proteomic analysis of the acid-soluble organic matrix  
633 of the chicken calcified eggshell layer. *Proteomics* **6**, 3801–3810.
- 634 [47] Nagai K, Yano M, Morimoto K, Miyamoto H. 2007 Tyrosinase localization in mollusc  
635 shells. *Comp Biochem Physiol* **146**, 207–214.

- 636 [48] Mann K, Edsinger E. 2014 The *Lottia gigantea* shell matrix proteome: re-analysis  
637 including MaxQuant iBAQ quantification and phosphoproteome analysis. *Proteome Sci*  
638 **12**, 28.
- 639 [49] Oliveri C, Peric L, Sforzini S, Banni M, Viarengo A, Cavaletto M. 2014 Biochemical and  
640 proteomic characterisation of haemolymph serum reveals the origin of the alkali-labile  
641 phosphate (ALP) in mussel (*Mytilus galloprovincialis*). *Comp Biochem Physiol Part D*  
642 *Genomics Proteomics* **11**, 29–36
- 643 [50] Treccani L, Mann K, Heinemann F, Fritz M. 2006 Perlwapin, an abalone nacre protein  
644 with three four-disulfide core (whey acidic protein) domains, inhibits the growth of  
645 calcium carbonate crystals. *Biophys J* **91**, 2601–2608.
- 646 [51] Liu HL, Liu SF, Ge YJ, Liu J, Wang XY, Xie LP, Zhang RQ, Wang Z. 2007  
647 Identification and characterization of a biomineralization related gene PFMG1 highly  
648 expressed in the mantle of *Pinctada fucata*. *Biochemistry* **46**, 844–851.
- 649 [52] Bédouet L, Duplat D, Marie A, Dubost L, Berland S, Rousseau M, Milet C, Lopez E.  
650 2007 Heterogeneity of proteinase inhibitors in the water-soluble organic matrix from the  
651 oyster nacre. *Mar Biotechnol* **9**, 437–449.
- 652 [53] Arivalagan J, Marie B, Sleight VA, Clark MS, Berland S, Marie A. 2016 Shell matrix  
653 proteins of the clam, *Mya truncata*: Roles beyond shell formation through proteomic study  
654 *Mar Genomics* **27**, 69-74.
- 655 [54] Dombre C, Guyot N, Moreau T, Monget P, Da Silva M, Gautron J, Réhault-Godbert S.  
656 2016 Eggsepins: The chicken and/or the egg dilemma. *Semin Cell Dev Biol* in press.  
657 <http://dx.doi.org/gate1.inist.fr/10.1016/j.semcdb.2016.08.019>
- 658 [55] Keith J, Stockwell S, Ball D, Remillard K, Kaplan D, Thannhauser T, Sherwood R. 1993  
659 Comparative analysis of macromolecules in mollusc shells. *Comp Biochem Physiol B* **105**,  
660 487-496.
- 661 [56] Giribet, G. 2008 Bivalvia In *Phylogeny and Evolution of the Mollusca*. (W. F. Ponder &  
662 D. R. Lindberg, ed. Berkeley) Berkeley: University of California Press, pp. 105-141.
- 663 [57] Chateigner D, Ouhenia S, Krauss C, Hedegaard C, Gil O, Morales M, Lutterotti L,  
664 Rousseau M, Lopez E. 2010 Voyaging around nacre with the X-ray shuttle: from bio-  
665 mineralisation to prosthetics via mollusc phylogeny. *Mater Sci Engin A* **528**, 37-51.
- 666 [58] Jackson DJ, Mann K, Häussermann V, Schilhabel M, Lüter C, Griesshaber E, Schmahl  
667 W, Wörheide G. 2015 The *Magellania venosa* biomineralizing proteome: a window into  
668 Brachiopod shell evolution. *Gen Bio Evol* **7**, 1349-1362.

- 669 [59] Luo Y, Takeushi T, Koyanagi R, Yamada L, Kanda M, Khalturine M, Fujie M,  
670 Yamasaki S, Endo K, Satoh N. 2015 The *Lingula* genome provides insights into  
671 brachiopod evolution and the origin of phosphate biomineralization. *Nature Comm* **6**,  
672 8301.
- 673 [60] Marin F, Layrolle P, De Groot K, Westbroek, P. 2003 The Origin of metazoan skeleton,  
674 in *Biomineralization: Formation, Diversity, Evolution and Application* (Kobayashi and H.  
675 Osawa, Eds.), Tokai University Press, Kanagawa. pp. 50–53.
- 676 [61] Le Roy N, Jackson D, Marie B, Ramos-Silva P, Marin F. 2014 The evolution of metazoan  
677  $\alpha$ -carbonic anhydrases and their roles in calcium carbonate. *Frontiers Zool* **11**:75.
- 678 [62] Leaf DS, Anstrom JA, Chin JE, Harkey MA, Showman RM, Raff RA. 1987 Antibodies  
679 to a fusion protein identify a cDNA clone encoding msp130, a primary mesenchyme-  
680 specific cell surface protein of the sea urchin embryo. *Dev Biol* **121**, 29-40.
- 681 [63] Harkey MA, Whietley HR, Whiteley HA. 1992 Differential expression of the msp130  
682 gene among skeletal lineage cells in the sea urchin embryo: a three dimensional *in situ*  
683 hybridization analysis. *Mech Dev* **37**, 173-184.
- 684 [64] Mann K, Wilt F, Poustka A. 2010 Proteomic analysis of sea urchin (*Strongylocentrotus*  
685 *purpuratus*) spicule matrix. *Proteome Sci* **8**, 33.
- 686 [65] Szabo R, Ferrier DE. 2015 Another biomineralising protostome with an msp130 gene  
687 and conservation of msp130 gene structure across Bilateria. *Evol Dev* **17**, 195-197.
- 688 [66] Tagliabracci V, Wiley S, Guo X, Kinch L, Durrant E, Wen J, Xiao J, Cui J, Nguyen K,  
689 Engel J, Coon J, Grishin N, Pinna L, Pagliarini D, Dixon J. 2015 A single Kinase generates  
690 the majority of the secreted phosphoproteome. *Cell* **161**, 1619-1632.
- 691 [67] Marin F, Bundeleva I, Takeuchi T, Immel F, Medakovic D. 2016 Organic matrices in  
692 metazoan calcium carbonate skeletons: composition, functions, evolution. *J Struct Biol* in  
693 press. DOI: 10.1016/j.jsb.2016.04.006
- 694 [68] Marie B, Ramos-Silva P, Marin F, Marie A. 2013 Proteomics of CaCO<sub>3</sub> biomineral-  
695 associated proteins: How to properly address their analysis. *Proteomics* **13**, 3109-3116.
- 696 [69] Arivalagan J, Yarra T., Marie B, Sleight V, Duvernois-Berthet E, Clark M, Marie A,  
697 Berland S. 2016 Insight from the shell proteome: biomineralization to adaptation. *Mol Biol*  
698 *Evol* in press. DOI: 10.1093/molbev/msw219
- 699 [70] Kelley L, Mezullis S, Yates C, Wass M, STengerg M. 2015 The Phyre2 web portal for  
700 protein modelling, prediction and analysis. *Nature protocols* **10**, 845-858.
- 701 [71] Zhang G, Fang X, Guo X, Luo R, Xu F, Yang P, Zhang L, Wang X, Qi H, Xiong Z, Que

702 H, Xie Y, Holland PW, Paps J, Zhu Y, Wu F, *et al.* 2012 The oyster genome reveals stress  
703 adaptation and complexity of shell formation. *Nature* **490**, 49-54.  
704 [72] Mann K, Jackson D. 2014 Characterization of pigmented shell-forming proteome of the  
705 common grove snail *Cepaea nemoralis*. *BMC Genomics* **15**:249.

706

## 707 **Figure legends**

708

709 **Figure 1.** Identification of the nacre matrix proteins from *Elliptio complanata* and *Villosa*  
710 *lienosa* shells using MS/MS analyses. Venn diagram of 41 and 38 proteins identified in both  
711 nacre matrices. The hashtag symbol (#) beside some protein names represents cases where the  
712 identification is not 100% certain, since it is based only on one peptide and only in one of the  
713 two species.

714

715 **Figure 2.** Schematic representation of the primary structure of unionoid extracellular matrix  
716 (ECM) nacre proteins retrieved from *Elliptio complanata* and/or *Villosa lienosa*. Each  
717 complete protein sequence possesses a signal peptide indicated in red. Typical ECM domains  
718 are indicated as boxes on the protein structure. The list of ECM protein domains comprises  
719 VWA, CBD2, LamG, Chitin\_binding\_3, EFh, CLECT, ANF\_receptor and  
720 FAM20C/DUF1193, together with few RLCs or repeated domains. The “?” symbol  
721 indicates missing sequence information.

722

723 **Figure 3.** Nacre SMPs from bivalve models. In total, 48, 35 and 42 various matrix proteins  
724 have already been detected in the nacre of the three bivalve models that belong to the  
725 Unionidae, Pteriidae and Mytilidae families, respectively. Names correspond to proteins  
726 and/or proteinaceous domains identified in the different nacre SMPs. <sup>p</sup> and <sup>m</sup> exponents  
727 indicate that the protein was also detected in the prismatic shell layer of either *Pinctada spp.*  
728 or *Mytilus spp.*, respectively [2;15;17;18].

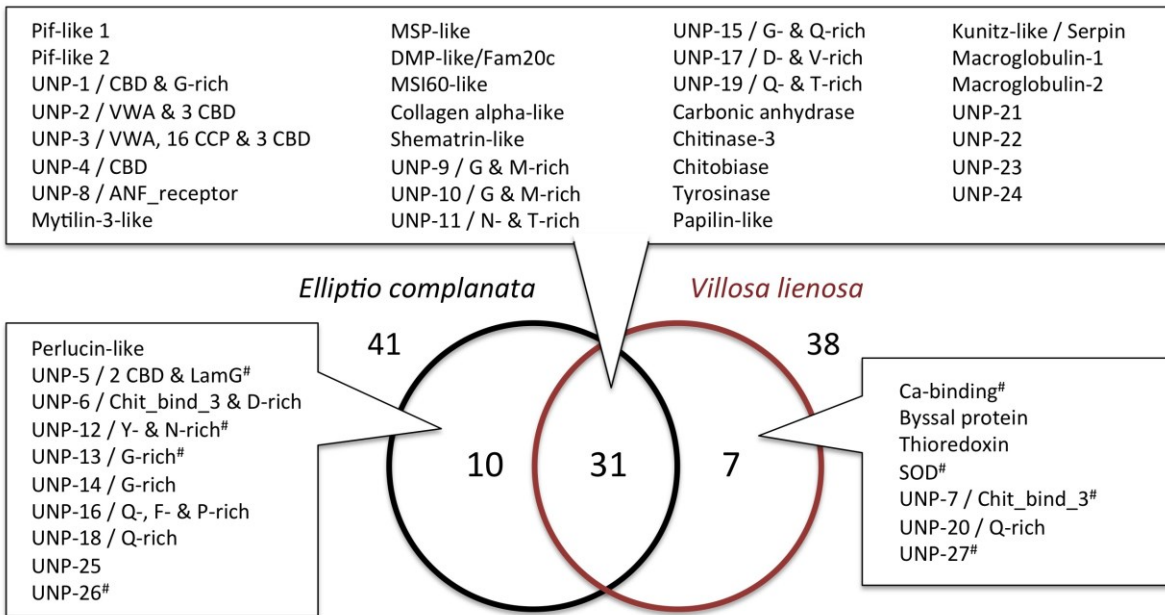
729

730 **Figure 4.** Comparison of SMP domain distribution in the shells of various lophotrochozoan  
731 models, focused on molluscs and brachiopods. The domains are sorted according to main  
732 categories detected in SMPs. \* indicates that only genuine abundant SMPs presenting high  
733 confidence for their specific identification in the shell matrix, and not being potential  
734 considered as contaminant have been mentioned here.

735

736

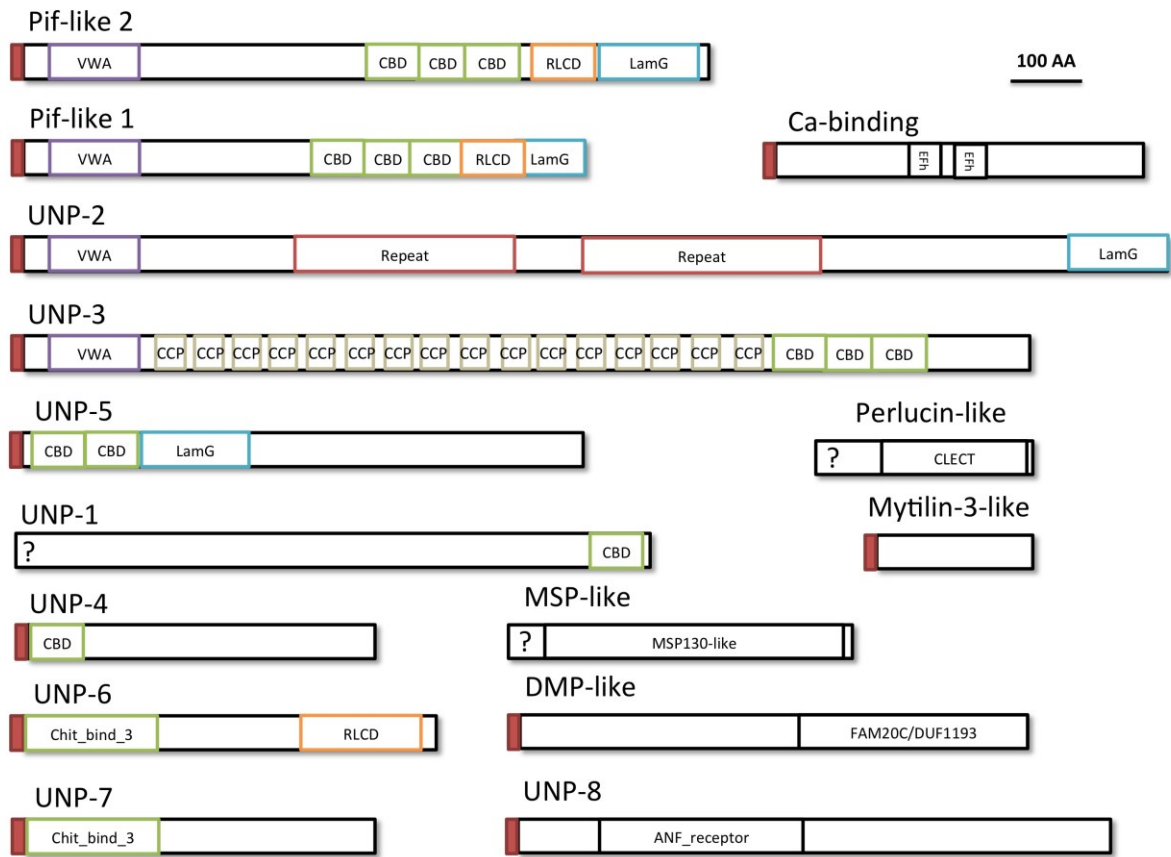
737



739

740

741

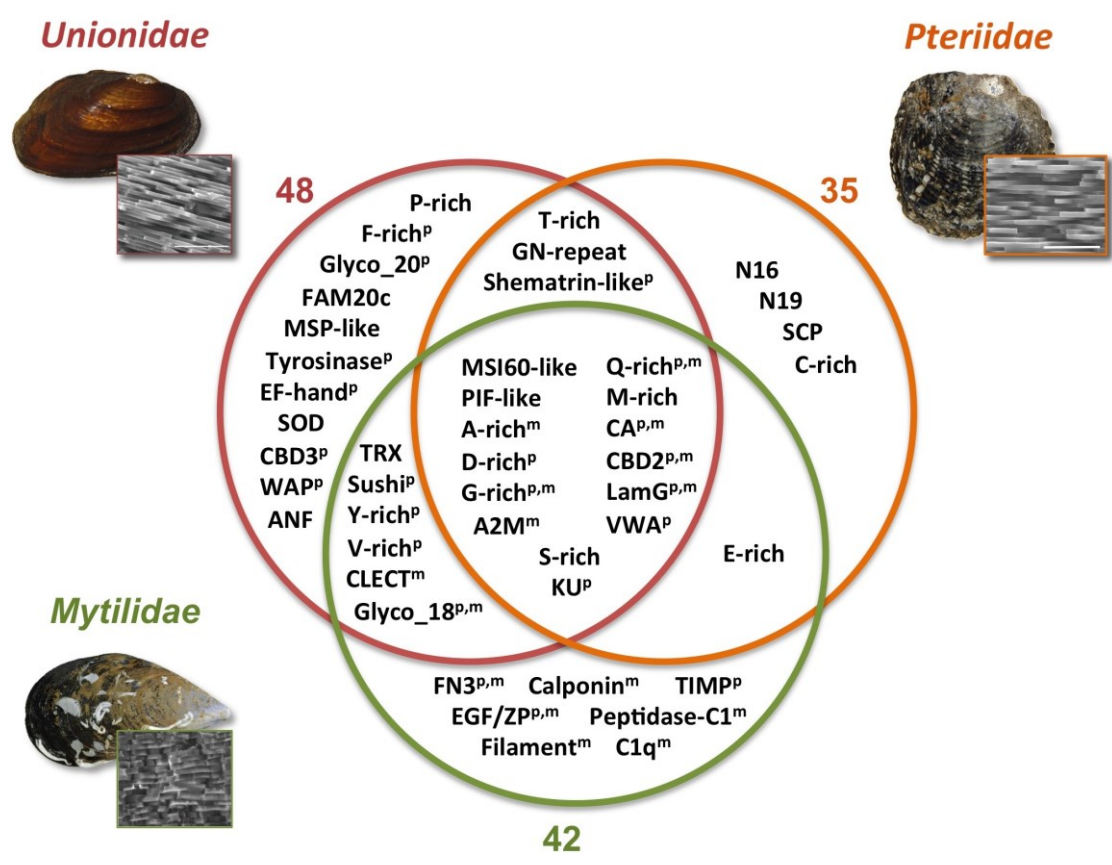


743

744

745

746 Fig. 3



747

748

749

